Nuclear Engineering and Technology 51 (2019) 1272–1278

Contents lists available at ScienceDirect

Nuclear Engineering and Technology

journal homepage: www.elsevier.com/locate/net

Original Article

An approach to the coupled dynamics of small lead cooled fast reactors

M. Zarei

Engineering Department, Shahid Beheshti University, P.O. Box: 1983969411, Tehran, Iran

ARTICLE INFO

Article history:
Received 20 July 2018
Received in revised form
23 February 2019
Accepted 20 March 2019
Available online 24 March 2019

Keywords:
Lead coolant
Natural circulation
Boussinesq approximation
Reduced order model
Nyquist stability

ABSTRACT

A lumped kinetic modeling platform is developed to investigate the coupled nuclear/thermo-fluid features of the closed natural circulation loop in a low power lead cooled fast reactor. This coolant material serves a reliable choice with noticeable thermo-physical safety characteristics in terms of natural convection. Boussienesq approximation is resorted to appropriately reduce the governing partial differential equations (PDEs) for the fluid flow into a set of ordinary differential equations (ODEs). As a main contributing step, the coolant circulation speed is accordingly correlated to the loop operational power and temperature levels. Further temporal analysis and control synthesis activities may thus be carried out within a more consistent state space framework. Nyquist stability criterion is thereafter employed to carry out a sensitivity analysis for the system stability at various power and heat sink temperature levels and results confirm a widely stable natural circulation loop.

1. Introduction

Inherent safety paradigms have gradually gained popularity in the realm of nuclear facilities [1]. This property basically alludes to specific functional designs which permanently maintain a process within safe boundary conditions [2]. A higher level of reliability is thus accrued from the application of passive mechanisms making use of the laws of nature and the need for external driving force or power supplies is excluded. As such, natural circulation phenomenon has long been actively pursued as a promising heat transport mechanism in energy conversion facilities [3]. This Buoyancy driven flow established as a result of the density gradient throughout the coolant loop has already been employed in certain innovative prototypes of Small Modular nuclear Reactors (SMR) [4]. Liquid metal coolants (i.e. sodium, lead or lead-bismuth alloy) have shown to serve as suitable choice in this respect for the future generation of nuclear power. The work presented herein takes into account the liquid lead with low working pressure and excellent heat transfer capabilities [5] as the case study.

Proper modeling and investigation of the stability features for the natural circulation loops remains however an ongoing issue and a comprehensive review thereof may be found in Ref. [3]. The governing mass, momentum and energy partial differential equations (PDEs) essentially give a space-time description of the coolant flow. An approach commonly adopted to explore the pertaining stability behavior relies on the assumption of an exponential perturbation ($\delta(t) = \varepsilon e^{\gamma t}$) for the equations around the nominal operating point [6]. This would help address the local stability behavior as a function of the space variable employing the Nyquist criterion. Low order dynamic modeling schemes which tend to recast these coupled PDEs into ordinary differential equations (ODEs) are nonetheless favored for further stability analysis or control synthesis purposes [7]. A rather rigorous approach [8,9] employs the Fourier synthesis framework as a space-time decomposition tool to generate a finite set of ODEs. Proper selection of the sufficient Fourier constituent terms is however a challenging issue. Despite simplifying assumptions, lumped kinetic schemes often give a reasonably accurate treatment of the natural circulation phenomenon. Coupled zero dimensional models have been developed in Refs. [10,11] for the core of water cooled research reactors and a more detailed study has been carried out in Ref. [12] for the primary circuit of a lead cooled research reactor. The effect of loop length on the establishment of a delayed flow rate has moreover been investigated in Refs. [13,14]. The work presented herein makes use of the Boussinesq approximation [3,15], to help interrelate the loop flow rate and the bulk temperatures and thus simplify the underlying equations. The manuscript is accordingly organized as follows: in the next section, basic physical modeling of the natural circulation loop is presented and a lumped kinetic model is derived

E-mail address: mo_zarei@sbu.ac.ir.

https://doi.org/10.1016/j.net.2019.03.015

Nomenclature

P	Reactor power
C	Delayed neutrons precursor density
Λ	Neutron mean generation time
λ_{eff}	Effective precursors time constant
β_{eff}	Effective delayed neutron fraction
K_D	Doppler constant
α_{ax}	Fuel axial expansion coefficient of reactivity
α_{Pb}	Coolant temperature coefficient of reactivity
α_{rad}	Core radial expansion coefficient of reactivity
H_r	Fuel column height
r_f	Pellet radius
$r_{c,i}$	Clad inner radius
$r_{c,o}$	Clad outer radius
d	fuel rod pitch
N_f	Number of pins
D_h	Hydraulic diameter
H_s	Steam generator height
H_h	Hot leg length
H_c	Cold leg length
H	vertical leg height
L	horizontal leg length
ρ_l	Lead density
β_l	Volumetric coefficient of thermal expansion (Lead)
$c_{p,l}$	Lead specific heat capacity
k_l	Lead thermal conductivity
μ_l	Lead dynamic viscosity
ν_l	Lead kinematic viscosity
ρ_c	Clad density
$c_{p,c}$	Clad specific heat capacity
k_c	Clad thermal conductivity
ρ_f	Fuel density
$c_{p,f}$	Fuel specific heat capacity
k_f	Fuel thermal conductivity
p	coolant pressure
T_i	Core inlet temperature
T_o	Core outlet temperature
T_s	Bulk temperature of the secondary coolant
T_f	Fuel Temperature
T_c	Clad Temperature
T_l	Coolant Temperature
A	Flow area per pin
h_{fc}	Fuel to clad heat transfer coefficient
h_{cl}	Clad to coolant heat transfer coefficient
Re	Reynolds number
Pr	Prandtl number
Pe	Peclet number
Nu	Nusslet number
f	Friction factor
v	coolant velocity

through certain simplifying assumptions quite reasonable for the small reactor under scrutiny. Simulation results for a perturbing input reactivity are moreover given in this coupled thermo-fluid natural circulation loop. A local linear stability analysis is carried out afterwards employing the Nyquist criterion for a set of models obtained at various nominal power levels and heat sink temperatures. Results confirm that the loop dynamic stability is maintained throughout a large power span. The dependence of the loop mass flux on the mentioned parameters (core power and the ambient temperature) is finally explored.

2. Model development

Fig. 1 displays a schematic of the closed natural circulation loop with the reactor core and the heat exchanger acting as the heater (source) and cooler (sink) sections respectively. This configuration with the sink placed above the source renders Bouyancy the sole driving force.

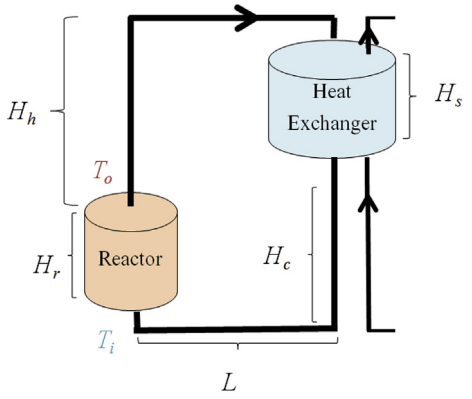

Fig. 1. The closed natural circulation loop.

A set of general assumptions are employed to further carry out a model reduction scheme on the loop conservation equations for the mass, momentum and energy [3,15].

I. A fully one dimensional model with no variation of the cross section.
II. All coolant properties are constant except for the fluid density which obeys the Boussinesq approximation. As such, all density terms are constant except for the one in the body force term of the momentum equation where $\rho = \rho_0[1 - \beta_l(T_l - T_{l,0})]$.
III. The connecting pipes are fully insulated thereby maintaining a constant temperature across the hot and the cold legs.
   a. *The mass conservation equation:* Employing the Boussinesq approximation helps assume the coolant velocity a space-independent variable (Eq. (1)).

$$\frac{\partial \rho}{\partial t} + \frac{\partial \rho v}{\partial z} = 0 \xrightarrow[\rho=\rho_0]{Boussiensq\ \text{Approximation}} v = v(t) \tag{1}$$

$$\frac{\partial \rho v}{\partial t} + \frac{\partial \rho v^2}{\partial z} = -\frac{\partial p}{\partial z} - \rho g \hat{z}.\hat{h} - \frac{1}{2}\frac{f}{D_h}\rho v^2 \xrightarrow{Boussiensq\ \text{Approximation}}$$

$$\rho_0 \frac{\partial v}{\partial t} + \rho_0 \frac{\partial v^2}{\partial z} = -\frac{\partial p}{\partial z} - \rho_0[1 - \beta_l(T - T_0)]g\hat{z}.\hat{h} - \frac{1}{2}\frac{f}{D}\rho_0 v^2 \tag{2}$$

   b. *The momentum conservation equation:* Similarly Eq. (2) is reformulated wherein $\hat{z}.\hat{h}$ stands for the dot product of the gravity unit vector $(\hat{z})$ and that of the loop length $(\hat{h})$ [3]. As such, it gives rise to a negative contribution on the hot leg and a positive contribution on the cold leg.

The above formula is integrated around the closed loop which would result in Eq. (3) with H and L representing the length of each of the vertical and horizontal leg respectively.

$$\rho_0 \oint \frac{\partial v}{\partial t} dz + \rho_0 \oint \frac{\partial v^2}{\partial z} dz = -\oint \frac{\partial p}{\partial z} - \oint \rho_0 [1 - \beta_l (T - T_0)] g \hat{z}.\hat{h} dz - \oint \frac{1}{2} \frac{f}{D} \rho_0 v^2 dz \Rightarrow$$
$$2(H + L) \frac{dv}{dt} = -\oint [1 - \beta_l (T - T_0)] g \hat{z}.\hat{h} dz - (H + L) \frac{f}{D} v^2 \quad (3)$$

The loop integral of pressure vanishes accordingly and the body force term is computed (Eq. (4)) taking into account the sign of the dot product $(\hat{z}.\hat{l})$.

$$-\oint \left[1 - \beta_l (T - T_0)\right] g \hat{z}.\hat{h} dz = -\int_0^H [1 - \beta_l (T - T_0)] g dz + \int_H^{2H} [1 - \beta_l (T - T_0)] g dz$$
$$= -\beta_l g \left(\int_0^H T dz - \int_H^{2H} T dz \right) = \int_0^{H_r} T dz + \int_{H_r}^{H_r + H_h} T dz - \int_{H_c}^{H_s + H_c} T dz - \int_0^{H_c} T dz \quad (4)$$

The above integral is simplified (Eq. (6)) assuming a linear temperature distribution throughout the small size core and the heat exchanger (Eq. (5)). The momentum conservation equation is eventually given in Eq. (7).

$$T_l \approx T_s \approx \frac{T_o + T_i}{2} \Rightarrow T_o = 2T_l - T_i \quad (5)$$

$$-\oint [1 - \beta_l (T - T_0)] g \hat{z}.\hat{h} dz = T_l H_r + T_o H_h - T_s H_s - T_i H_c \xrightarrow{Eq.5} = \underbrace{(H_r + 2H_h - H_s)}_{\gamma_l} T_l + (-H_h - H_c) \gamma_i T_i \quad (6)$$

$$2(H + L) \frac{dv}{dt} = -\beta_l g (\gamma_l T_l + \gamma_i T_i) - (H + L) \frac{f}{D} v^2 \quad (7)$$

$$m_f c_{p,f} \frac{dT_f}{dt} = \frac{P}{N_f} - h_{fc} \left(T_f - T_c \right) \quad (8)$$

$$m_c c_{p,c} \frac{dT_f}{dt} = h_{fc} \left(T_f - T_c \right) - h_{cl} (T_c - T_l) \quad (9)$$

$$m_l c_{p,l} \frac{dT_l}{dt} = h_{cl} (T_c - T_l) + (\dot{m}_i h_i - \dot{m}_o h_o) = h_{cl} (T_c - T_l) + \rho_o c_{p,l} v A (T_i - T_o) \xrightarrow{Eq.5} m_l c_{p,l} \frac{dT_l}{dt} = 2\rho_o v A c_{p,l} (T_i - T_l) + h_{cl} (T_c - T_l) \quad (10)$$

$$m_s c_{p,l} \frac{dT_i}{dt} = (\dot{m}_o h_o - \dot{m}_i h_i) - h_s (T_i - T_s) = c_{p,f} \rho_o v A (T_o - T_i) - h_s (T_i - T_s) \xrightarrow{Eq.5} m_s c_{p,l} \frac{dT_i}{dt} = 2\rho_o v A c_{p,l} (T_l - T_i) - h_s (T_i - T_s) \quad (11)$$

Table 1
Design data for the natural circulation loop [12,17].

P_0(nominal)	0.5 MW	α_l	$-0.43 \times 10^{-5}K^{-1}$	T_w	500 K	H_s	0.48 m
Λ	$50 \times 10^{-9}s$	α_{rad}	$-1.54 \times 10^{-5}K^{-1}$	r_f	5.75 mm	H_h	1.77 m
H_r	0.3 m	A	$4.849 \times 10^{-5}m^2$	$r_{c,i}$	5.80 mm	H_c	1.77 m
λ_{eff}	$8 \times 10^{-2}s^{-1}$	$c_{p,c}$	563.1 J/kg.K	$r_{c,o}$	6.3 mm	ρ_c	7731 kg/m^3
β_{eff}	267×10^{-5}	k_c	20.04 W/m.K	d	14 mm	ρ_f	9486 kg/m^3
K_D	-6×10^{-5}	k_f	13.5 W/m.K	N_f	397		
α_{ax}	$-0.70 \times 10^{-5}K^{-1}$	$c_{p,f}$	637.6 J/kg.K	D_h	4.211 mm		

c. *The Energy conservation equations:* Corresponding equations are respectively given in Eq. (8) to Eq. (10) with the Boussinesq approximation taken for granted accordingly. The model comprises a single fuel rod, the cladding area and the associated channel for the lead coolant to further pass through the heat exchanger. The heat transfer through the heat exchanger is moreover represented in Eq. (11) wherein a bulk temperature is assumed for the secondary coolant (T_s).

A point kinetic description of the neutron balance equations within the core which comprises both abrupt and delayed fissions is given in Eq. (12) to Eq. (15). The control rod external reactivity (ρ_{ext}) which modulates the fission reaction rate and the generated heat acts as the system external driving force. The counter-acting temperature reactivity feedback (ρ_{fb}) comprises terms due to the Doppler broadening, axial fuel expansion, coolant thermal expansion and the grid radial expansion associated to variations of the inlet coolant temperature. These temperature feedbacks give rise to quite reliable inherent safety mechanisms in liquid metal cooled fast reactors [16].

$$\frac{dP}{dt} = \frac{\rho_{net} - \beta_{eff}}{\Lambda} P + \lambda_{eff} C \tag{12}$$

$$\frac{dC}{dt} = \frac{\beta_{eff}}{\Lambda} P - \lambda_{eff} C \tag{13}$$

$$\rho_{net} = \rho_{ext} + \rho_{fb} \tag{14}$$

$$\rho_{fb} = K_D \ln\left(T_f / T_{f,0}\right) + \alpha_{ax}\left(T_f - T_{f,0}\right) + \alpha_l\left(T_l - T_{l,0}\right) + \alpha_{rad}\left(T_{in} - T_{in,0}\right) \tag{15}$$

Concurrent solution of Eq. 7 through 13 reflects the dynamic behavior of the nuclear coupled natural circulation loop. Steady (permanent) behavior is readily obtained for $\rho_{ext} = 0$.

3. Simulation and analysis

Design data for the primary circuit of the lead cooled nuclear research facility operating at the atmospheric pressure are given in Table 1.

Correlations given in Table 2 are applied to compute coolant properties wherein definitions for the Peclet number ($Pe = Re \times Pr$), the Prandtl number ($\mathrm{Pr} = \mu c_p/k$), the Reynolds number ($\mathrm{Re} = \rho v D/\mu$), and the dynamic viscosity $\mu[m^2/s] = \nu/\rho$ are employed for the coolant.

Besides, the corresponding bulk heat transfer coefficients are given through Eqs. (16) and (17) [10] wherein the heat capacity of the coolant is given $h[W/m^2.K] = Nu \times k/D_h$.

$$h_{fc} = \frac{1}{\frac{1}{4\pi H_c k_f} + \frac{\ln(r_{c,i}/r_f)}{2\pi H_c k_c}} \tag{16}$$

$$h_{cl} = \frac{1}{\frac{\ln(r_{c,out}/r_{c,i})}{2\pi H_c k_c} + \frac{1}{h_l A}} \tag{17}$$

Simulation results are given hereafter for a 50 pcm (i.e. 50×10^{-5} [δk/k]) input reactivity insertion due to control rod displacement which respectively display the normalized core output power (Fig. 2), the core net reactivity (Fig. 3), the fuel, clad, coolant and input temperatures (Fig. 4) and the coolant circulation speed throughout the core (Fig. 5). The step input reactivity results in a consequent change in the power and the corresponding temperatures and is accordingly balanced through certain fluctuations (Figs. 2 and 3). A new quiescent operating point is therefore obtained following this reactivity insertion practice. An almost 1000 s settling time is figured out for the nuclear coupled natural circulation loop. The delay induced by the coolant transport throughout the circulation loop [13,14] is not accounted for in this work and may be rigorously addressed employing more refined models (e.g. the two node framework[1]). A rule of thumb analysis in this regard however reveals that while oscillations caused by an input reactivity perturbations maintain a 200 [s] period (Figs. 2–5) the average flow velocity (Fig. 4) for the coolant is almost $v = 0.24[m/s]$ which incur a loop delay of $\tau \approx 2(H_s + H_c)/v \approx 20[s]$ (neglecting the connecting pipes length). Input reactivity perturbations thus evolve on a quite slower basis (almost 10 times) than the coolant transport delay. It is therefore quite plausible to assume that oscillation modes induced due the loop transition delay do not practically interfere with those set out by the structural feedback effects, and may be reasonably disregarded in this study. The in-phase oscillating behavior of temperature profiles (Fig. 5) is likewise reasonably attributed to neglecting the core transport delay.

3.1. Stability analysis

A sensitivity analysis with regards to the core operating power (P_0) and the sink temperature (T_s) is moreover carried out for the nonlinear system described in Eq. (7) to Eq. (12). To this end the stability behavior of a pertaining open loop transfer function $[\delta P(s)/\delta\rho_{ext}(s)]$ is investigated in terms of the Nyquist frequency response for various quiescent operating powers and sink temperatures separately. Nyquist criterion derived from Cauchy's theory of conformal mapping postulates that in order to maintain input/output stability of a transfer function the so called Nyquist plot (real vs. imaginary graph in the complex plane) should not encircle the origin [6]. This would help examine the local stability at several

[1] The author has already submitted a manuscript to investigate the effect of delay induced instability due to coolant circulation employing the two node layout for a specific type of GEN-IV reactors.

Table 2
Basic thermo-physical correlations for the lead coolant [18].

$\rho_l[kg/m^3] = (11.42 - 12.42 \times 10^{-4}T_l) \times 10^3$	$\nu_l[Pa.s] = (15.87 \times 10^3/T_l - 2.65) \times 10^{-8}$
$c_{p,l}[J/kg.K] \simeq 147.3$	$f = 1.139/\mathrm{Re}^{0.35324}$
$k_l[W/m.K] = 15.8 + 108 \times 10^{-4}(T_l - 600.4)$	$Nu = 4.0468 + .0162Pe^{0.77}$

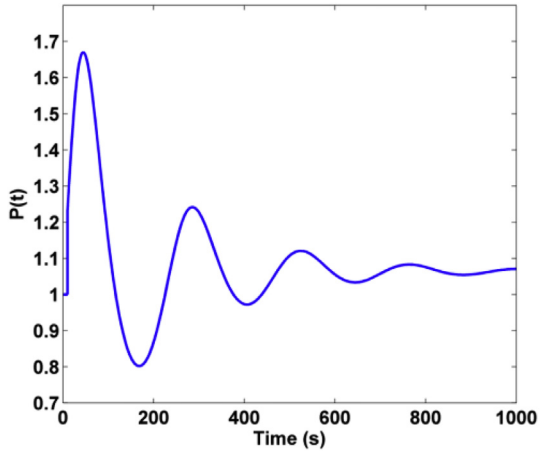

Fig. 2. Core power profile.

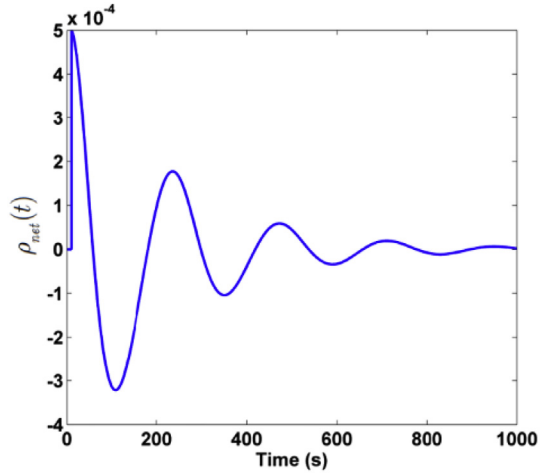

Fig. 3. Resultant reactivity of the core.

operating points. The local Jacobian system is characterized in Eq. (18) following the framework described in Fig. 6 for a generic representation of a control affine nonlinear system (Eqs. (7)–(12)). The associated state vector, state transition, input and output matrices are given in Eq. (19)–(23). Input reactivity due to the control rod manipulation acts as the model input ($u = \rho_{ext}$). The model transfer function at the nominal operating point is given by Eq. (23).

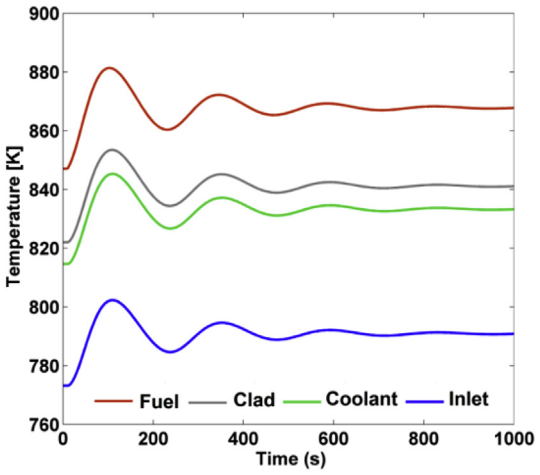

Fig. 4. Temperature profiles in the loop.

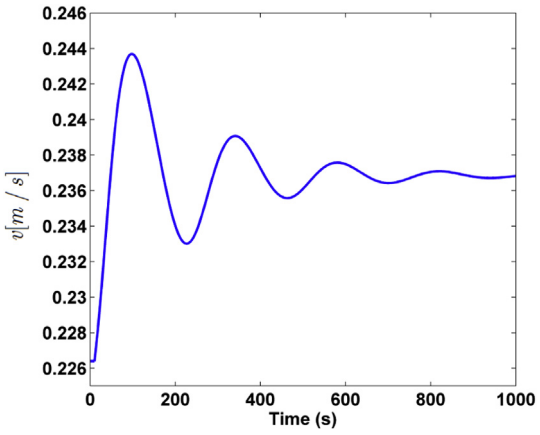

Fig. 5. Coolant velocity profile.

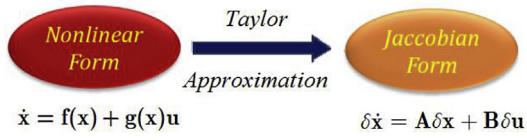

Fig. 6. The local linearization framework.

$$\dot{\mathbf{x}} = \mathbf{f}(\mathbf{x}) + \mathbf{g}(\mathbf{x})\mathbf{u} \rightarrow \delta\dot{\mathbf{x}} = \left(\frac{\partial \mathbf{f}}{\partial \mathbf{x}} + \frac{\partial \mathbf{g}}{\partial \mathbf{x}}\right)\Big|_{\mathbf{x}_0} \delta\mathbf{x} + \mathbf{g}(\mathbf{x}_0)\delta\mathbf{u} = \mathbf{A}\delta\mathbf{x} + \mathbf{B}\delta\mathbf{u} \tag{18}$$

$$\delta\mathbf{x} = \begin{bmatrix} \delta P & \delta C & \delta T_f & \delta T_c & \delta T_l & \delta T_i & \delta v \end{bmatrix}^T \tag{19}$$

$$A=\begin{bmatrix} \frac{-\beta_{eff}}{\Lambda} & \frac{\beta_{eff}}{\Lambda} & \frac{K_D}{T_{f0}}+\alpha_{ax} & 0 & \frac{\alpha_l}{\Lambda} & \frac{\alpha_{rad}}{\Lambda} & 0 \\ \lambda_{eff} & -\lambda_{eff} & 0 & 0 & 0 & 0 & 0 \\ \frac{P_0}{N_f m_f c_{p,f}} & 0 & \frac{-h_{fc}}{m_f c_{p,f}} & \frac{h_{fc}}{m_f c_{p,f}} & 0 & 0 & 0 \\ 0 & 0 & \frac{h_{fc}}{m_c c_{p,c}} & \frac{-\left(h_{fc}+h_{cl}\right)}{m_c c_{p,c}} & \frac{h_{cl}}{\left(m_c c_{p,c}\right)} & 0 & 0 \\ 0 & 0 & 0 & \frac{h_{cl}}{m_c c_{p,l}} & \frac{-\left(h_{cl}+2v_0 A c_{p,l}\rho_{l,0}\right)}{\left(m_l c_{p,l}\right)} & \frac{2v_0 A c_{p,l}\rho_{l,0}}{m_l c_{p,l}} & \frac{-2A c_{p,l}\rho_{l,0}\left(T_{l,0}-T_{i,0}\right)}{m_l c_{p,l}} \\ 0 & 0 & 0 & 0 & \frac{2v_0 A c_{p,l}\rho_{l,0}}{m_s c_{p,l}} & \frac{\left(-2v_0 A c_{p,l}\rho_{l,0}-h_s\right)}{m_s c_{p,l}} & \frac{2A c_{p,l}\rho_{l,0}\left(T_{l,0}-T_{i,0}\right)}{m_s c_{p,l}} \\ 0 & 0 & 0 & 0 & \frac{-\beta_l g\gamma_l}{2(H+L)} & \frac{-\beta_l g\gamma_i}{2(H+L)} & \frac{-f v_0}{D_h} \end{bmatrix} \tag{20}$$

$$\mathbf{B}=[1/\Lambda \quad 0 \quad 0 \quad 0 \quad 0 \quad 0 \quad 0]^T \tag{21}$$

$$H(s)=\frac{\delta P(s)}{\delta \Sigma_{a2}(s)}=C(SI-A)^{-1}B\Rightarrow$$
$$H_{\text{nominal}}=\frac{2\times 10^7(s+2.342)(s+0.1979)(s+0.08)(s+0.003333)\left(s^2+3.394s+1556\right)}{\left(s+5.34\times 10^4\right)(s+2.343)(s+0.1944)\left(s^2+0.009301s+0.0006628\right)\left(s^2+3.394s+1556\right)} \tag{23}$$

$$\mathbf{C}=[1 \quad 0 \quad 0 \quad 0 \quad 0 \quad 0 \quad 0] \tag{22}$$

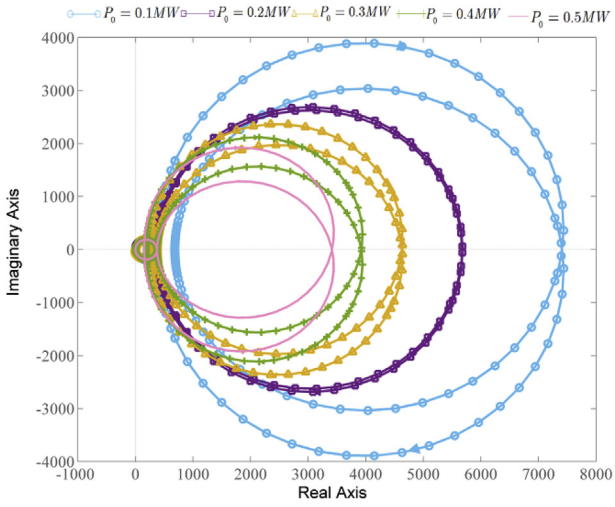

Fig. 7. Nyquist plot for local models (as a function of P_0).

Graphs for the Nyquist plots are demonstrated in Figs. 7 and 8 respectively for the core operating power ($0.1MW < P_0 < 0.5MW$) and the sink temperature ($100K < T_s < 500K$) taken as the variable (scheduling) parameters. No encirclement of the origin is figured out which thereby predicates a stable natural circulation loop. Likewise, variations of mass flux in the closed natural circulation loop are displayed in Figs. 9 and 10. The mass flux increases with the heat source (reactor) power whereas it decreases with the sink temperature. Raising the source power at a fixed sink temperature gives rise to a higher temperature (density) gradient between the source and sink. This would give rise to a growth of loop mass flux and a more pronounced natural circulation. Increasing the sink temperature at a fixed source power on the other hand, results in a lower temperature (density) gradient among these two points and thus incurs a reduction in the loop mass flux.

4. Conclusion

This work has presented a reduced order framework to investigate the coupled thermo-neutronic behavior of a closed natural circulation loop. To this effect, a research type lead cooled fast nuclear reactor is adopted as the case study and the coupled nuclear/thermo-fluid equations are explored as a nonlinear dynamic system. On the basis of the Boussinesq approximation, the

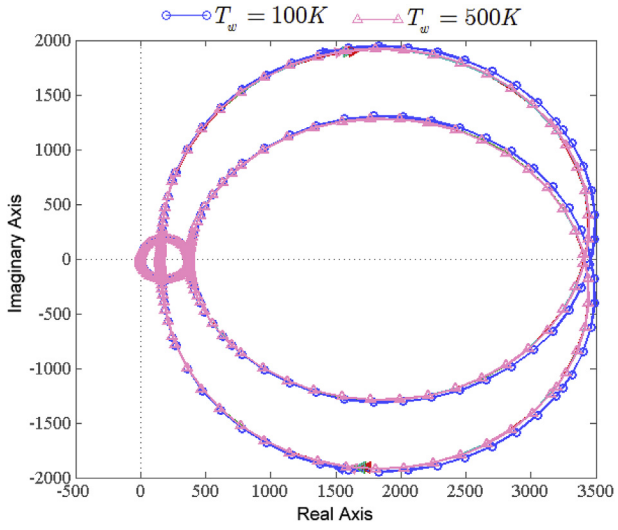

Fig. 8. Nyquist plot for the local models (as a function of T_s).

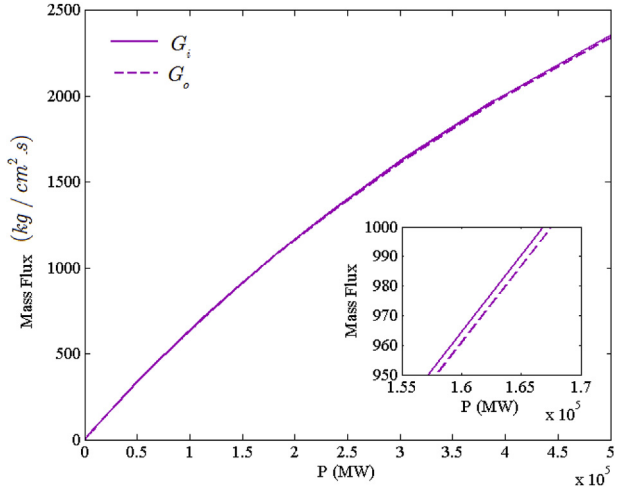

Fig. 9. Variation of the loop mass flux by the reactor power.

governing PDE Navier-Stokes equations are reasonably recast into equivalent ordinary differential equations (ODE). As such, the coolant circulation speed is correlated to the loop operational power and temperature levels which would eventually yield a compact thermo-neutronic model quite suitable for stability and control purposes. The Nyquist criterion is thereafter employed which indicates stable natural circulation loops for various operating points as a function of source (reactor) power and the sink (ambient) temperature. Besides, the loop mass flux reflects direct and reverse dependence on these two parameters respectively which is physically justified by their impact on the temperature (density) gradient within the loop.

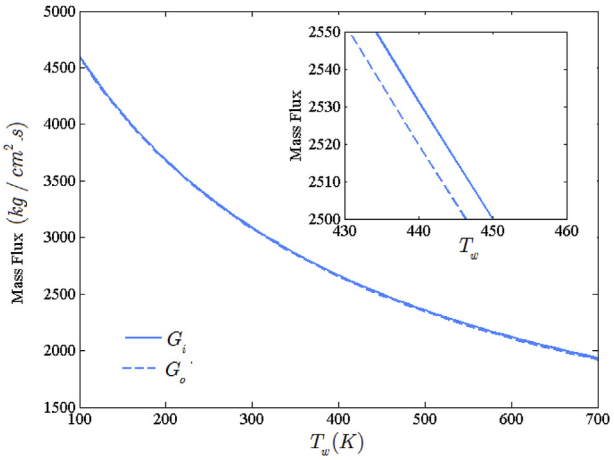

Fig. 10. Variation of the loop mass flux by the sink temperature.

References

[1] D.T. Ingersoll, Deliberately small reactors and the second nuclear era, Prog. Nucl. Energy 51 (2009) 589–603.
[2] H. van Dam, Physics of nuclear reactor safety, Rep. Prog. Phys. 11 (1992) 2025–2077.
[3] Y. Zvirin, A review of natural circulation loops in pressurized water reactors and other systems, Nucl. Eng. Des. 67 (1981) 203–225.
[4] J. Vujic, R.M. Bergmann, R. Skoda, M. Miletic, Small modular reactors: simpler, safer, faster? Energy 43 (2012) 288–295.
[5] L. Cinotti, C.F. Smith, H. Sekimoto, L. Mansani, M. Reale, J.J. Sienicki, Lead cooled system design and challenges in the frame of Generation IV international forum, J. Nucl. Mater. 415 (2011) 245–253.
[6] Q. Wu, J.J. Sienicki, Stability analysis on single phase natural circulation in Argonne lead loop facility, Nucl. Eng. Des. 224 (2003) 23–32.
[7] H.-X. Li, C. Qi, Modeling of distributed parameter systems for applications- a synthesized review from time-space separation, J. Process Control 20 (2010) 891–901.
[8] D. Lu, X. Zhnag, C. Guo, Stability analysis for single phase liquid metal rectangular natural loops, Ann. Nucl. Energy 73 (2014) 189–199.
[9] M. Gorman, P.J. Widmann, K.A. Robbins, Nonlinear dynamics of a convective loop: a quantitative comparison of experiment with theory, Physica D 19 (1986) 255–267.
[10] A. Cammi, R. Ponciroli, A.B. di Trigliole, G. Magrotti, M. Prata, D. Chiesa, E. Previtali, A zero dimensional model for simulation of TRIGA Mark II dynamic response, Prog. Nucl. Energy 68 (2013) 43–54.
[11] K. Ardaneh, S. Zaferanlouei, A lumped parameter core dynamics model for the MTR type research reactors under natural convection regime, Ann. Nucl. Energy 56 (2013) 243–250.
[12] S. Bortot, E. Suvdantsetseg, J. Wallenius, BELLA: a multi-point dynamic code for safety-informed design of fast reactors, Ann. Nucl. Energy 85 (2015) 228–235.
[13] Y.M. Farawila, D.R. Todd, M.J. Ades, J.N. Reyes, Analytical stability analogue for single phase natural circulation loop, Nucl. Sci. Eng. 184 (2016) 321–333.
[14] V. Casamassima, P. Colombo, S. Canevese, Preliminary study on a plant control structure for GEN-IV fast reactor, Proc. IFAC 18 (2011) 3734–3740.
[15] S. Nadella, A.K. Srivastava, N.J. Maheshwari, A semi-analytical model for linear stability analysis of rectangular natural circulation loops, Chem. Eng. Sci. 192 (2018) 892–905.
[16] D.C. Wade, E.K. Fujita, The integral fast reactor concept: physics of operation and safety, Nucl. Sci. Eng. 100 (1988) 507–524.
[17] J. Wallenius, E. Suvdantsetseg, Electra: european lead cooled training reactor, Nucl. Technol. 177 (2012) 303–313.
[18] Thermo-physical properties of materials for nuclear engineering: a tutorial and collection of data, Int. Atom. Energy Agency (2008) 81–118.